Journal of Mineralogical and Petrological Sciences, Volume 100, page 229–236, 2005

Distribution of Fe^{3+} in a synthetic $(Ca,Na)_2(Mg,Fe^{3+})Si_2O_7$-melilite: ^{57}Fe Mössbauer and X-ray Rietveld studies

Masahide AKASAKA*, Mariko NAGASHIMA*, Kuniaki MAKINO** and Haruo OHASHI***

*Department of Materials Creation Technology, Graduate School of Science and Engineering, Shimane University, 1060 Nishikawatsu, Matsue 690-8504, Japan
**Department of Geology, Faculty of Science, Shinshu University, Asahi 3-1-1, Matsumoto 390-8621, Japan
***1-9-25 Nishinakanobe, Shinagawa-Ku, Tokyo 142-0054, Japan

Crystal structure and the ^{57}Fe Mössbauer spectrum of synthetic $(Ca_{1.53}Na_{0.47})(Mg_{0.52}Fe^{3+}_{0.49})Si_{1.99}O_7$-melilite have been investigated to confirm the location of Fe^{3+} at the *T1* site, and to evaluate the effect of an incommensurate structure on ^{57}Fe Mössbauer hyperfine parameters. A conventional Rietveld refinement with occupancies of Ca(*W*), Na(*W*), Mg(*T1*), Fe^{3+}(*T1*) and Si(*T2*) fixed to 0.765, 0.235, 0.515, 0.485 and 2.00, respectively, converged well with an R_{wp} (*R*-weighted pattern) of 13.14% and a goodness-of-fit of 1.337, indicating exclusive Fe^{3+} distribution at the *T1* site. However, the Mössbauer spectrum consists of two doublets with an isomer shift of 0.19 mm/s and quadrupole splitting of 0.75 and 1.04 mm/s, which can be attributed to Fe^{3+} at the *T1* site. There are two sorts of *T1* site with distinguishable distortion in the synthetic Na-Fe^{3+}-melilite, which might be attributed to the existence of an incommensurate phase at room temperature.

Keywords: Melilite, Mössbauer, X-ray Rietveld, Ferric iron, Synthetic mineral, Crystal structure

INTRODUCTION

Melilite group minerals have tetragonal, $P\bar{4}2_1m$, symmetry, with one sort of 8-coordinated site (*W*) and two sorts of tetrahedral sites (*T1* and *T2*). In the åkermanite ($Ca_2MgSi_2O_7$)-type melilite, divalent cations such as Mg^{2+}, Fe^{2+}, Zn^{2+} etc., occupy the *T1* site, and Si^{4+} the *T2* site (Warren, 1930; Warren and Trautz, 1930; Smith, 1953; Ito and Peiser, 1969; Louisnathan, 1969; Kimata and Ii, 1981; Kimata and Ohashi, 1982; Kimata, 1982, 1983a, 1983b), whereas, in the gehlenite ($Ca_2AlAlSiO_7$)-type melilite, the *T1* site is filled with trivalent cations (M^{3+}), and the *T2* site is occupied by $M^{3+}_{1.0}Si_{1.0}$ (Louisnathan, 1970). On the other hand, in the sodamelilite ($NaCaAlSi_2O_7$)-type melilite, M^{3+} and Si^{4+} occupy *T1* and *T2* sites, respectively (Louisnathan, 1970).

Akasaka and Ohashi (1985) and Akasaka et al. (1986) studied the distribution of Fe^{3+} in synthetic melilites using the Mössbauer method, and assigned one ^{57}Fe Mössbauer doublet of $(Na,Ca)_2(Mg,Fe^{3+})Si_2O_7$-melilite to Fe^{3+} at the *T1* site, and two doublets of synthetic melilites containing Fe^{3+}-bearing gehlenite type components to the *T1* and *T2* sites. Following those studies, Seifert et al. (1987) found an incommensurate structure in synthetic iron-åkermanite. Consequently, Seifert (1988) suggested that the two ^{57}Fe Mössbauer doublets reported by Akasaka and Ohashi (1985) and Akasaka et al. (1986) should be attributed to Fe^{3+} at the *T1* site, each exhibiting a different distortion. However, systematic study to evaluate the effect of an incommensurate structure in melilite on the ^{57}Fe Mössbauer hyperfine parameters of Fe^{3+} has not been carried out.

In this study, we have refined the crystal structure of synthetic $(Ca,Na)_2(Mg,Fe^{3+})Si_2O_7$-melilite to confirm the location of Fe^{3+} at the *T1* site and re-examined the ^{57}Fe Mössbauer spectrum to evaluate the effect of an incommensurate structure on Fe^{3+} Mössbauer hyperfine parameters.

EXPERIMENTAL METHODS

The sample used in this study is the same as that synthesized by Akasaka and Ohashi (1985): a mixture of $Na_2Si_2O_5$, $CaCO_3$, MgO, Fe_2O_3 and SiO_2 with a composition of $(Ca_2MgSi_2O_7)_{50}(NaCaFe^{3+}Si_2O_7)_{50}$ (mol%) was sintered at 1000 ºC for 30 days. The resulting crystallized melilite coexists with a very small amount of parawollastonite and a trace amount of hematite. According to Akasaka and Ohashi (1985), the composition was 42.7(6)

M. Akasaka, akasaka@riko.shimane-u.ac.jp Corresponding author
M. Nagashima, s039707@matsu.shimane-u.ac.jp
K. Makino, makinox@gipac.shinshu-u.ac.jp

SiO_2, 13.9(6) Fe_2O_3, 7.6(3) MgO, 30.8(4) CaO and 5.2(2) wt% Na_2O, which gives an average formula of $(Ca_{1.53}Na_{0.47})_{\Sigma 2.00}(Mg_{0.52}Fe^{3+}_{0.49})_{\Sigma 1.01}Si_{1.99}O_7$ (hereafter, Na-Fe^{3+}-melilite). The synthetic product was aggregates of rounded grains. Since grinding the sample to very small-sized particles is one of the most critical stages of any structural study based on powder X-ray diffraction data (Bish and Reynolds, 1989; Post and Bish, 1989), the product was finely ground using a hand agate mortar and pestle under alcohol for about 60 minutes. Using an optical microscope for examination, the particle size was kept below 10 μm.

The ^{57}Fe Mössbauer spectrum was measured at room temperature, using 370 MBq ^{57}Co in Pd as a source. The absorber was about 100 mg of finely ground sample. The Mössbauer data were obtained using a constant acceleration spectrometer fitted with a 1024 channel analyzer. The isomer shift was referred to a standard metallic iron foil. The Doppler velocity was calibrated with respect to the same standard. The spectrum was fitted to Lorentzians using the least squares method with line widths and intensities constrained to be equal at each site. The QBMOSS program of Akasaka and Shinno (1992) was used for computer analysis. The quality of the fit was judged using the χ^2 value and standard deviations of Mössbauer parameters.

The fine powder sample was mounted on a glass holder with a 20 × 18 × 0.5 mm cavity. The powder was densely packed from the back of the mount against a frosted glass slide giving a flat surface level with the top of the holder. Mounts for the intensity profile collection were made by loading the powder from the front of the holder. Following the method of Raudsepp et al. (1990), the surface was finely serrated several times with a razor blade. This method tends to randomize the orientation of any anisotropic crystals that are aligned during filling, while maintaining a generally flat surface.

Step scan powder diffraction data were collected using a RIGAKU RINT automated Bragg-Brentano diffractometer system equipped with incident- and diffracted-beam Soller slits, 1° divergence and scatter slits, a 0.15 mm receiving slit and a curved graphite diffracted-beam monochromator. The Cu X-ray tube generator was operated at 35 kV and 25 mA. The profile was taken between 10° and 130° in 2θ using a step interval of 0.05° and a step counting time of 2 seconds.

The crystal structure of the synthesized melilite was refined using the Rietveld program RIETAN-2000 (Izumi and Ikeda, 2000). The peaks were defined using the 'Modified split pseudo-Voigt' function, which comprised the split pseudo-Voigt function of Toraya (1990) combined with profile relaxation; an asymmetry parameter is built into this profile function. Details of the 'Modified split pseudo-Voigt' function are described in Izumi and Ikeda (2000). The preferred orientation was corrected with the March-Dollase function (Dollase, 1986). Since the product contained not only melilite but also a very small amount of parawollastonite, the structural parameters and mass fractions of melilite and parawollastonite were refined. The single crystal X-ray results for synthetic soda melilite $CaNaAlSi_2O_7$ (Louisnathan, 1970) and parawollastonite (Trojer, 1968) were used as initial parameters for the Rietveld refinement in our study. The cell parameters determined using a unit-cell parameter refinement program in the RIGAKU RINT system were used as the initial values. A nonlinear least-squares calculation using the Marquardt method was followed by the conjugate-direction method to check the convergence at a local minimum (Izumi, 1993).

RESULTS

Mössbauer spectroscopy

The Mössbauer hyperfine parameters are listed in Table 1. Akasaka and Ohashi (1985) fitted a spectrum of Na-Fe^{3+}-

Table 1. Mössbauer hyperfine parameters* of the $(Ca_{1.53}Na_{0.47})(Mg_{0.52}Fe^{3+}_{0.49})Si_{1.99}O_7$-melilite

Fitting	*I. S.* (mm/s)	*Q. S.* (mm/s)	*Γ* (mm/s)	Area ratio (%)	χ^2/Freedom	Assignment
One doublet						
	0.188(1)	0.947(2)	0.463(2)	-	1.89	Fe^{3+}(*T1*)
Two doublets						
AA'	0.187(1)	0.749(2)	0.303(4)	23(5)	1.10	Fe^{3+}(*T1*)
BB'	0.190(1)	1.04(2)	0.457(8)	77(8)		Fe^{3+}(*T1*)

* Standard deviations, 1σ, are given in parentheses.
I.S. isomer shift referred to a metallic iron absorber.
Q.S. quadrupole splitting.
Γ Full width at half height.

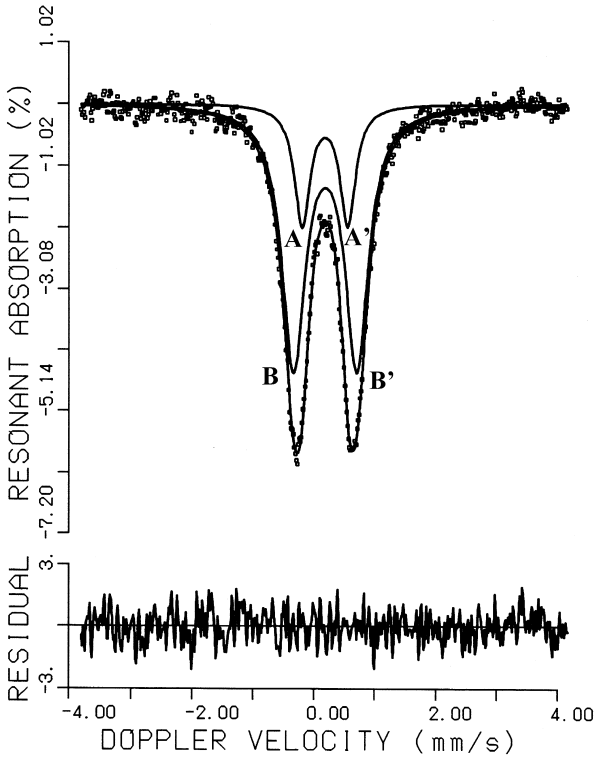

Figure 1. Mössbauer spectrum of synthetic $(Ca_{1.53}Na_{0.47})(Mg_{0.52}Fe^{3+}_{0.49})Si_{1.99}O_7$–melilite at room temperature.

melilite with one doublet attributed to Fe^{3+}(*T1*). However, in the present study, one doublet fit resulted in a large chi-square value of 1.89 χ^2/Freedom, but the two doublets fit produced a reasonable chi-square value of 1.10 χ^2/Freedom (Fig. 1). Taking the chemical formula of Na-Fe^{3+}-melilite, $(Ca_{1.53}Na_{0.47})_{\Sigma 2.00}(Mg_{0.52}Fe^{3+}_{0.49})_{\Sigma 1.01}Si_{1.99}O_7$, into consideration, both doublets AA′ and BB′ are attributed to Fe^{3+} at the *T1* site. This assignment indicates the existence of two sorts of *T1* site in Na-Fe^{3+}-melilite. Since the quadrupole splitting (*Q.S.*) depends on the site distortion (Bancroft et al., 1967), the *T1* tetrahedra showing the Fe^{3+} Mössbauer doublet with the smaller *Q.S.* are more regular in shape than those with the larger *Q.S.*

Rietveld refinement

To confirm the restricted distribution of Fe^{3+} at the *T1* site in the Na-Fe^{3+}-melilite, Fe occupancies were refined not only at the *T1* site but also at the *T2* site in a preliminary Rietveld refinement. As a result, Fe at the *T2* site was not detected. In the final refinement, occupancies of Ca(*W*), Na(*W*), Mg(*T1*), Fe^{3+}(*T1*) and Si(*T2*) were fixed to 0.765, 0.235, 0.515, 0.485 and 2.00, respectively, on the basis of chemical composition. The refined powder patterns are shown in Figure 2, where the incommensurate structure

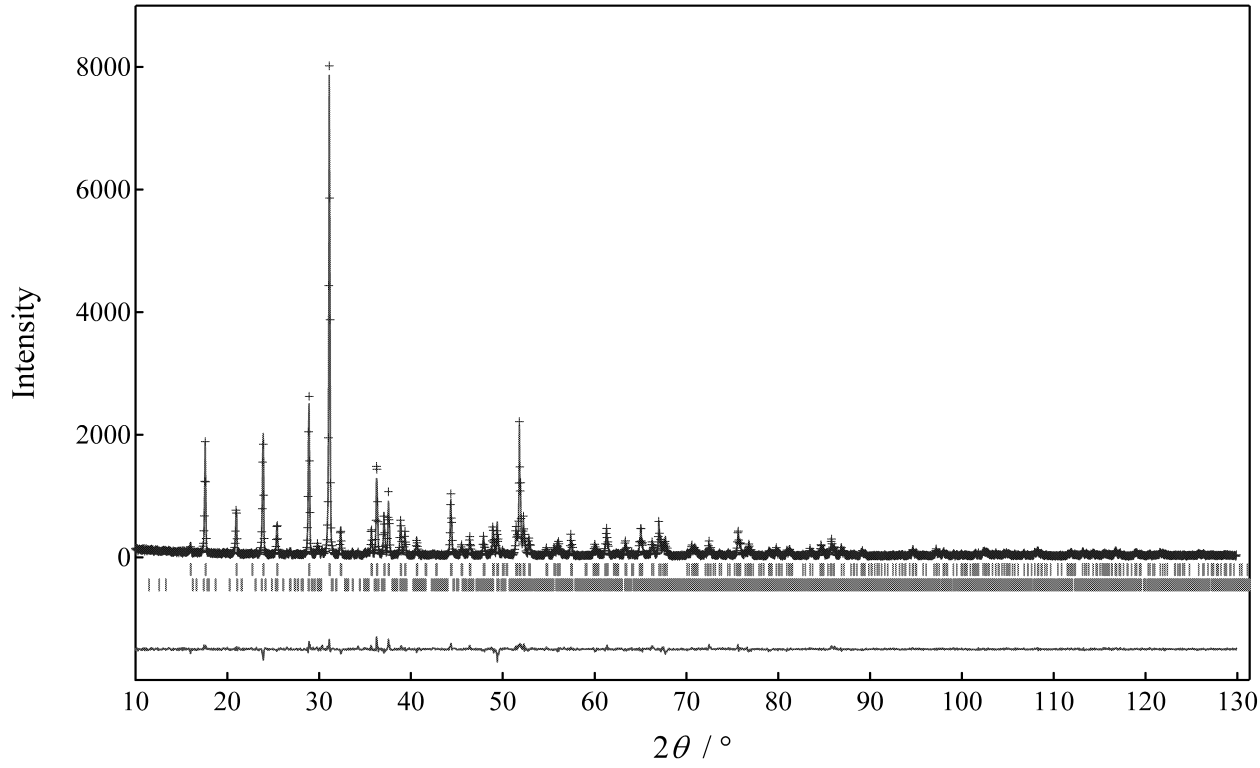

Figure 2. Observed and calculated X-ray powder diffraction pattern for the synthetic $(Ca_{1.53}Na_{0.47})(Mg_{0.52}Fe^{3+}_{0.49})Si_{1.99}O_7$–melilite refined in space group $P\bar{4}2_1m$. The crosses are the observed data, the solid line is the calculated pattern, and the vertical bars mark all possible Bragg reflections ($K\alpha_1$ and $K\alpha_2$) for melilite and parawollastonite (below). The difference between the observed and calculated patterns is shown at the bottom.

Table 2. Data collection and details of structure refinement

2θ scan range (°)	10 – 130	
Step interval (°2θ)	0.05	
Integration time/step (s)	2	
Max. intensity (counts)	8017	
No. of phase refined	2	
Phase	Melilite	Parawollastonite
Chemical formula	$Ca_{1.53}Na_{0.47}Mg_{0.52}Fe^{3+}_{0.49}Si_2O_7$	$CaSiO_3$
Crystal system	Tetragonal	Monoclinic
Space group	$P\bar{4}2_1/m$	$P2_1/a$
a (Å)	7.8228(2)	15.477(9)
b (Å)	7.8228(2)	7.375(3)
c (Å)	5.0271(1)	7.064(3)
β (°)		95.39(5)
V (Å^3)	307.64(1)	802.7 (7)
Z	2	12
D_{calc} (g/cm^3)	3.023	2.883
No. of unique reflections	98	1468
No. of refined parameters	183	
$[N-P]$*[1]	2217	
R_p (%)*[2]	9.48	
R_{wp} (%)*[2]	13.14	
R_e (%)*[2]	9.83	
S*[2]	1.337	
R_B (%)*[2]	3.64	3.12
R_F (%)*[2]	2.45	1.70
D–W d *[3]	1.331	1.383
r *[4]	1.201	1.136
Mass fraction	0.957	0.043

*[1] No. of observations (steps) – no. of refined parameters.
*[2] R_p, R-pattern; R_{wp}, R-weighted pattern; R_e, R-expected; S, Goodness-of-fit (= R_{wp}/R_e); R_B, R-Bragg factor; R_F, R-structure factor (Young, 1993).
*[3] Durbin-Watson d statistic (Hill and Flack, 1987).
*[4] Preferred-orientation parameter in the March-Dollase function.

Table 3. Refined atomic positions and temperature factors

	Multiplicity	Wyckoff letter	Occupancy	Coordinates			B*[1]
				x	y	z	
O1	4	e	1.00	1/2	0	0.173(2)	3.3(6)
O2	2	a	1.00	0.1468(9)	1/2-x	0.250(1)	3.3(6)
O3	4	e	1.00	0.0801(7)	0.1865(9)	0.798(1)	3.0(6)
CaNa	2	c	Ca0.765Na0.235	0.3351(3)	1/2-x	0.1865(9)	2.3(5)
MgFe	4	e	Mg0.515Fe0.485	0	0	0	2.0(5)
Si	8	f	1.00	0.1374(3)	1/2-x	0.9386(6)	1.9(5)

*[1] Isotropic displacement parameters in Å^2.

was not taken into consideration. The R-factors (Young, 1993), goodness-of-fit indicator S (Young, 1993), Durbin-Watson d statistic (D-W d) (Hill and Flack, 1987), and preferred orientation parameter r in the March-Dollase function and mass fractions of melilite and parawollastonite are shown in Table 2. The final results are characterized by R_{wp} (R-weighted pattern) = 13.14%, S = 1.337 and D-W d of 1.331 for the refinement of melilite. In terms of S, the fit between the observed and calculated patterns is acceptable. The mass fractions of melilite and

Table 4. Interatomic distances (Å) and selected interatomic angles (°)

T1 –O3 [4×]	1.885(6)	*W*–O3 [2×]	2.477(6)
Mean *T1*–O	1.885	*W*–O2	2.454(6)
O3–O3' [2×]	3.176(9)	*W*–O1	2.482(7)
O3–O3" [4×]	3.028(7)	*W*–O3"" [2×]	2.718(6)
O3–*T1*–O3' [2×]	114.8(2)	*W*–O2' [2×]	2.729(7)
O3–*T1*–O3" [4×]	106.9(2)	O2–*W*–O3 [2×]	69.2(1)
		O3–*W*–O3'	2.8(1)
T2–O1	1.620(4)	O2–*W*–O3' [2×]	82.4(1)
T2–O2	1.569(5)	O2'–*W*–O3'	80.8(1)
T2–O3 [2×]	1.612(7)	O1–*W*–O2'"[2×]	105.4(2)
O1–O2	2.676(9)	O1–*W*–O3'" [2×]	58.1(2)
O1–O3 [2×]	2.535(5)	O3'"–*W*–O3""	150.7(2)
O3–O3'	2.582(8)		
O3–O2 [2×]	2.671(7)		
T2–O1–*T2'*	139.5(4)		
O1–*T2*–O2	114.3(1)		
O1–*T2*–O3 [2×]	103.3(3)		
O3–*T2*–O3'"	106.4(3)		
O3–*T2*–O2 [2×]	114.2(3)		
T2–O3–*T1*	121.2(2)		

parawollastonite were 0.957 and 0.043, respectively.

Refined atom positional parameters and isotropic atomic displacement parameters are shown in Table 3. Interatomic distances (Å) and selected interatomic angles (°) are listed in Table 4.

DISCUSSION

As well as the result by Akasaka and Ohashi (1985), the exclusive distribution of Fe^{3+} at the *T1* site in synthetic Na–Fe^{3+}–melilite was confirmed in the present study by using the Mössbauer and Rietveld methods. Moreover, we found that Na–Fe^{3+}–melilite has two sorts of *T1* sites with different degrees of distortion, which resulted from the ^{57}Fe Mössbauer spectrum with two doublets assigned to Fe^{3+} at the *T1* site. Seifert et al. (1987) found a similar phenomenon in Fe^{2+}–bearing åkermanite with their Mössbauer study, and concluded that the incommensurate phase exhibits two distinguishable *T1* sites containing Mg and Fe^{2+}. Moreover, the existence of a low–temperature incommensurate phase in åkermanite has been confirmed by electron microscopic and electron diffraction studies (Seifert et al., 1987; Iishi et al., 1989, 1990), ^{29}Si MAS NMR (magic–angle spinning nuclear magnetic resonance) spectroscopy (Merwin et al., 1989), EXAFS analyses (Tamura et al., 1996), X–ray single crystal structure refinement (Kimata and Saito, 1987; Armbruster et al., 1990; Hagiya et al., 1992, 1993; Kusaka et al., 1998) and other means (cf. Seifert and Röthlisberger, 1993). Thus, the reason for two *T1* sites with distinguishable distortions in the Na–Fe^{3+}–melilite might be attributed to the incommensurate structure at room temperature.

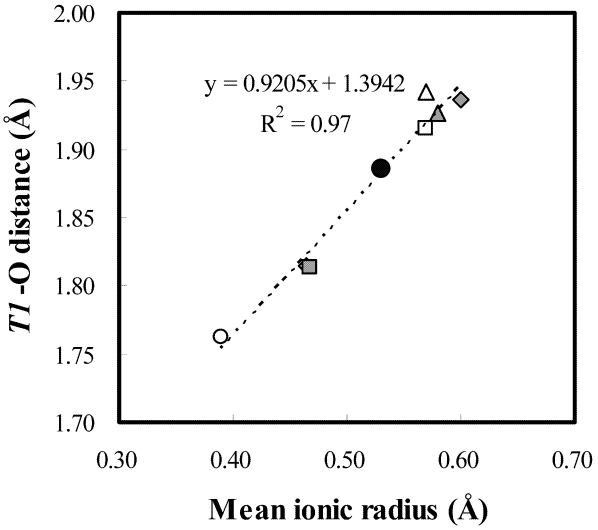

Figure 3. Variation of *T1*–O distance (Å) against mean ionic radius (Å). Filled circle, the $(Ca_{1.53}Na_{0.47})(Mg_{0.52}Fe^{3+}_{0.49})Si_{1.99}O_7$–melilite in this study; Gray diamond, $Ca_2ZnSi_2O_7$ (Louisnathan, 1969); Open circle, $CaNaAlSi_2O_7$ (Louisnathan, 1970); Open square, $Ca_2MgSi_2O_7$ (Kimata and Ii, 1981); Gray triangle, $Ca_2CoSi_2O_7$ (Kimata, 1983a); Open triangle, $Sr_2MgSi_2O_7$ (Kimata, 1983b); Open diamond and gray square, Sr–Na–melilite (Bindi et al., 2001).

The *Q.S.* values of Fe^{3+} at the two *T1* sites obtained in the present study, 0.749 and 1.04 mm/s, are important for the interpretation of the Mössbauer spectra of melilite. Akasaka and Ohashi (1985) and Akasaka et al. (1986)

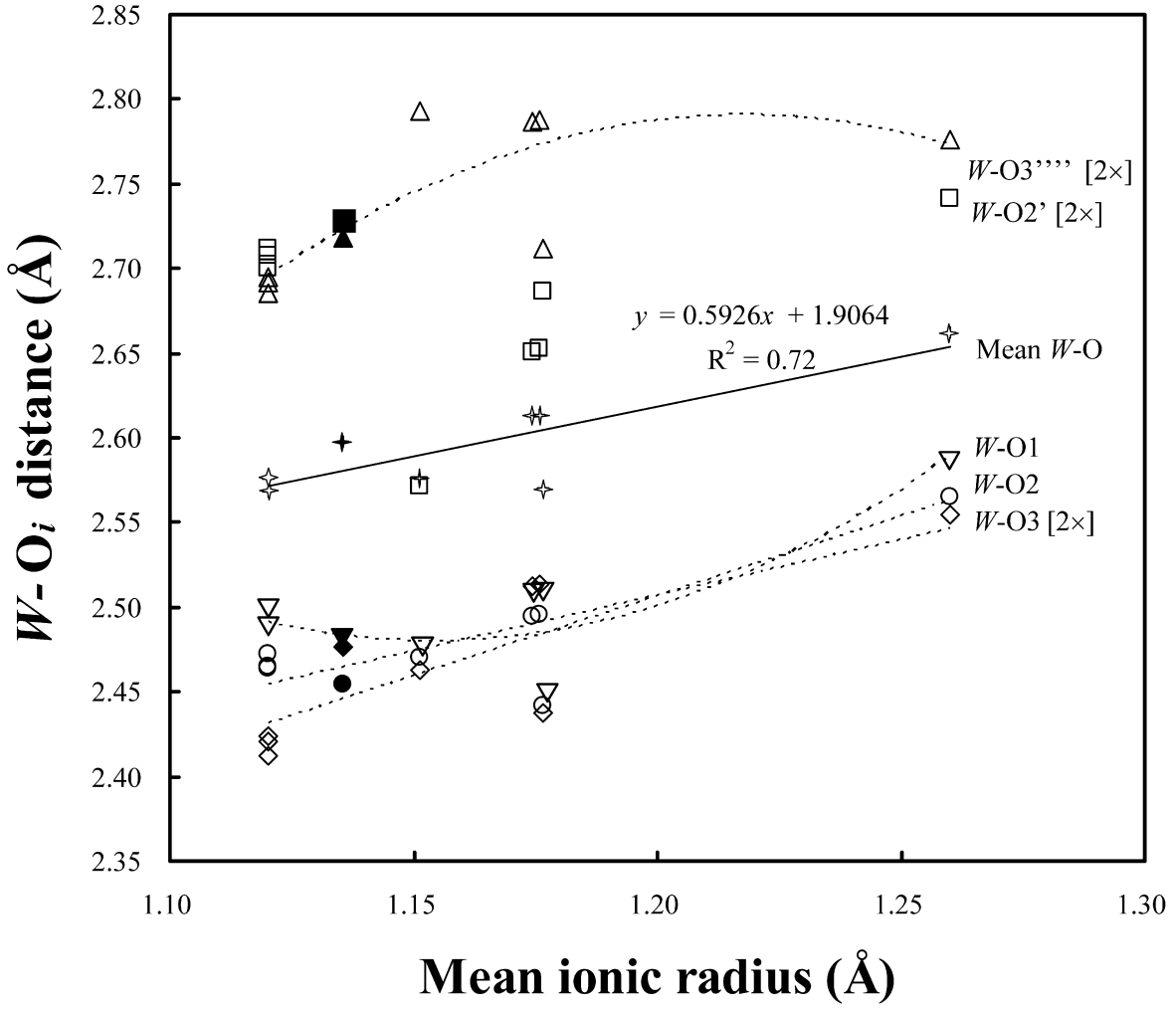

Figure 4. Variation of *W*–O*i* distances (Å) against mean ionic radius (Å). Filled marks represent the $(Ca_{1.53}Na_{0.47})(Mg_{0.52}Fe^{3+}_{0.49})Si_{1.99}O_7$–melilite in this study, and open marks are melilites reported so far: $Ca_2ZnSi_2O_7$ (Louisnathan, 1969), $CaNaAlSi_2O_7$ (Louisnathan, 1970), $Ca_2MgSi_2O_7$ (Kimata and Ii, 1981), $Ca_2CoSi_2O_7$ (Kimata, 1983a), $Sr_2MgSi_2O_7$ (Kimata, 1983b), and Sr–Na–melilite (Bindi et al., 2001). Reverse triangle, *W*–O1; Circle, *W*–O2; Square, *W*–O2'; Diamond, *W*–O3; Triangle, *W*–O3''''; Star, mean *W*–O.

found two Fe^{3+}–doublets in the ^{57}Fe Mössbauer spectra of synthetic melilites containing $Ca_2Fe^{3+}AlSiO_{7-}$, $Sr_2Fe^{3+}AlSiO_{7-}$, or $Ca_2Fe^{3+}GaSiO_7$–components, and assigned an inner doublet with a *Q.S.* of 0.8–1.3 mm/s to Fe^{3+}(*T1*) and an outer one with a *Q.S.* of 1.8–1.9 mm/s to Fe^{3+}(*T2*). Later, Seifert (1988) mentioned that both doublets should be assigned to Fe^{3+} at the *T1* sites with different distortions. However, the *Q.S.* values of the outer doublets assigned to Fe^{3+}(*T2*) by Akasaka and Ohashi (1985) and Akasaka et al. (1986) are too large to be attributed to Fe^{3+}(*T1*) in terms of the *Q.S.* values of Fe^{3+}(*T1*) of Na–Fe^{3+}–melilite in the present study (0.749 and 1.04 mm/s).

The exclusive distribution of Fe^{3+} at the *T1* site in Na–Fe^{3+}–melilite is also proven by the expression of the *T1*–O distance against the mean ionic radius at the *T1* site. As shown in Figure 3, the *T1*–O distance can be positively correlated to the mean ionic radius with the equation of <*T1*–O> (Å) = 0.9205 × [mean atomic radius (Å)]$_{T1}$ + 1.3942 (Å); the *T1*–O distance of Na–Fe^{3+}–melilite lies on this trend at the mean ionic radius derived from the occupancy of $Mg_{0.515}Fe^{3+}_{0.485}$ at the *T1* site.

As in other melilites, the *W* site of Na–Fe^{3+}–melilite shows four short *W*–O bonds and four long bonds (Fig. 4). Our result and the published data indicate that the mean *W*–O distance increases with increasing mean ionic radius at the *W* site, which is represented by the equation of <*W*–O> (Å) = 0.5926 × [mean atomic radius (Å)]$_W$ + 1.9064 (Å) (Fig. 4). The *W*–O1, –O2, –O3 and –O3'''' distances also tend to increase with increasing mean ionic radius. However, the *W*–O2' distances are very variable and do not seem to correlate with the mean ionic radius. It is noted that the *W*–O2' distance of $NaCaAlSi_2O_7$–melilite

of 2.572 Å given by Louisnathan (1970) is considerably smaller than those of other melilites.

The *T2*–O1, –O2 and –O3 distances are consistent with those of other melilites, in which the *T2* site is filled with Si, refined by X–ray single crystal structure analyses.

ACKNOWLEDGMENTS

The authors thank Dr. Fujio Izumi of the National Institute for Materials Science for his permission to use and help in using the RIETAN–2000 program. We are grateful to Dr. Shotaro Morimoto and an anonymous referee for their constructive reviews.

REFERENCES

Akasaka, M. and Ohashi, H. (1985) ^{57}Fe Mössbauer study of synthetic Fe^{3+}–melilites. Physics and Chemistry of Minerals, 12, 13–18.

Akasaka, M., Ohashi, H. and Shinno, I. (1986) The distribution of Fe^{3+} and Ga^{3+} between two tetrahedral sites in melilites, $Ca_2(Mg,Fe^{3+},Ga,Si)_3O_7$. Physics and Chemistry of Minerals, 13, 152–155.

Akasaka, M. and Shinno, I. (1992) Mössbauer spectroscopy and its recent application to silicate mineralogy. Journal of Mineralogical Society of Japan, 21, 3–20 (In Japanese with English abstract).

Armbruster, T., Röthlisberger, F. and Seifert, F. (1990) Layer topology, stacking variation, and site distortion in melilite–related compounds in the system $CaO–ZnO–GeO_2–SiO_2$. American Mineralogist, 75, 847–858.

Bancroft, G.M., Maddock, A.G. and Burns, R.G. (1967) Applications of the Mössbauer effect to silicate mineralogy – I. Iron silicates of known crystal structure. Geochimica et Cosmochimica Acta, 31, 2219–2246.

Bindi, L., Bonazzi, P. and Fitton, G. (2001) Crystal chemistry of strontian soda melilite from nepheline lava of Mt.Etinde, Cameroon. European Journal of Mineralogy, 13, 121–125.

Bish, D.L. and Reynolds, R.C. (1989) Sample preparation for X–ray diffraction. In Modern Powder Diffraction (Bish, D.L. and Post, J.E. Eds.). pp. 369, Reviews in Mineralogy, 20, Mineralogical Society of America, Washington DC, 73–99.

Dollase, W.A. (1986) Correction of intensities for preferred orientation in powder diffractometry: application of the March model. Journal of Applied Crystallography, 19, 267–272.

Hagiya, K., Ohmasa, M. and Iishi, K. (1992) Modulation of Co–åkermanite. Proceedings of the Japan Academy, 68, Ser. B, 25–29.

Hagiya, K., Ohmasa, M. and Iishi, K. (1993) Modulated structure of synthetic Co–åkermanite, $Ca_2CoSi_2O_7$. Acta Crystallographica, B49, 172–179.

Hill, R.J. and Flack, H.D. (1987) The use of the Durbin–Watson *d* statistic in Rietveld analysis. Journal of Applied Crystallography, 20, 356–361.

Iishi, K., Fujimoto, K. and Fujino, K. (1989) Single crystal growth of åkermanites $Ca_2Mg_{1-x}Co_xSi_2O_7$ with modulated structure. Neues Jahrbuch für Mineralogie Monatshefte, H.5, 219–226.

Iishi, K., Fujino, K. and Furukawa, Y. (1990) Electron microscopy studies of akermanites $(Ca_{1-x}Sr_x)_2CoSi_2O_7$ with modulated structure. Physics and Chemistry of Minerals, 17, 467–471.

Ito, J. and Peiser, H.S. (1969) Distorted tetrahedra in strontium copper åkermanite. Journal of Research of the National Bureau of Standards. Section A, Physics and Chemistry, 73A, 69–74.

Izumi, F. (1993) Rietveld analysis programs RIETAN and PREMOS and special applications. In the Rietveld Method (Young, R.A. Ed.). pp. 298, Oxford University Press, Oxford, UK, 236–253.

Izumi, F. and Ikeda, T. (2000) A Rietveld–analysis program RIETAN–98 and its application to zeolites. Material Science Forum, 321–324, 198–203.

Kimata, M. (1982) Four–coordinated Co^{2+} in $Ca_2CoSi_2O_7$. Naturwissenshaft, 69, 40–41.

Kimata, M. (1983a) The crystal structure and stability of Co–åkermanite, $Ca_2CoSi_2O_7$, compared with the mineralogical behavior of Mg cation. Neues Jahrbuch für Mineralogie Abhandlungen, 146, 221–241.

Kimata, M. (1983b) The structure properties of synthetic Sr–åkermanite: $Sr_2MgSi_2O_7$. Zeitschrift für Kristallographie, 163, 295–304.

Kimata, M. and Ii, N. (1981) The crystal structure of synthetic åkermanite, $Ca_2MgSi_2O_7$. Neues Jahrbuch für Mineralogie Abhandlungen, 144, 254–267.

Kimata, M. and Ohashi, H. (1982) The crystal structure of synthetic gehlenite, $Ca_2Al_2SiO_7$. Neues Jahrbuch für Mineralogie Abhandlungen, 143, 202–222.

Kimata, M. and Saito, S. (1987) Crystal structure of åkermanite at high temperature. 1987 year Joint Meeting of the Mineralogical Society of Japan, the Society of Resource Geology and the Japanese Association of Mineralogists, Petrologists and Economic Geologists. Abstracts, 39 (In Japanese).

Kusaka, K., Ohmasa, M., Hagiya, K., Iishi, K. and Haga, N. (1998) On variety of the Ca coordination in the incommensurate structure of synthetic iron–bearing åkermanite, $Ca_2(Mg_{0.55},Fe_{0.45})Si_2O_7$. Mineralogical Journal, 20, 47–58.

Louisnathan, S.J. (1969) Refinement of the crystal structure of hardystonite, $Ca_2ZnSi_2O_7$. Zeitschrift für Kristallographie, 130, 427–437.

Louisnathan, S.J. (1970) The crystal structure of synthetic soda melilite, $CaNaAlSi_2O_7$. Zeitschrift für Kristallographie, 131, 314–321.

Merwin, L.H., Sebald, A. and Seifert, F. (1989) The incommensurate–commensurate phase transition in akermanite, $Ca_2MgSi_2O_7$, observed by in–situ ^{29}Si MAS NMR spectroscopy. 16, 752–756.

Post, J.E. and Bish, D.L. (1989) Rietveld refinement of crystal structures using powder X–ray diffraction data. In Modern Powder Diffraction (Bish, D.L. and Post, J.E. Eds.). pp. 369, Reviews in Mineralogy, 20, Mineralogical Society of America, Washington DC, 73–99.

Raudsepp, M., Hawthorne, F.C. and Turnock, A.C. (1990) Evaluation of the Rietveld method for the characterization of fine–grained products of mineral synthesis: the diopside–hedenbergite join. Canadian Mineralogist, 28, 93–109.

Seifert, F. (1988) Recent advances in the mineralogical applications of the ^{57}Fe Mössbauer effect. In Proceedings of the NATO Advanced Study Institute on Physical Properties and Thermodynamic Behavior of Minerals (Salje, E.K.H. Ed.). pp. 707, D. Reidel Publishing Company, Dordrecht, Netherlands, 687–703.

Seifert, F., Czank, M., Simons, B. and Schmahl, W. (1987) A commensurate–incommensurate phase transition in iron–bearing åkermanites. Physics and Chemistry of Minerals, 14, 26–35.

Seifert, F. and Röthlisberger, F. (1993) Macroscopic and structural changes at the incommensurate–normal phase transition in melilites. Mineralogy and Petrology, 48, 179–192.

Smith, J.V. (1953) Reexamination of the crystal structure of melilite. American Mineralogist, 38, 643–661.

Tamura, T., Yoshiasa, A., Iishi, K., Takeno, S., Maeda, H., Emura, S. and Koto, K. (1996) Local structure of $(Ca,Sr)_2(Mg,Co,Zn)Si_2O_7$ melilite solid–solution with modulated structure, Physics and Chemistry of Minerals., 23, 81–88.

Toraya, H. (1990) Array–type universal profile function for powder pattern fitting. Journal of Applied Crystallography, 23, 485–491.

Trojer, F.J. (1968) The crystal structure of parawollastonite. Zeitschrift für Kristallographie 127, 291–308.

Young, R.A. (1993) Introduction to the Rietveld method. In the Rietveld Method (Young, R.A. Ed.). pp. 298, Oxford University Press, Oxford, UK, 1–38.

Warren, B.E. (1930) The structure of melilite $(Ca,Na)_2(Mg,Al)_1(Si,Al)_2O_7$. Zeitschrift für Kristallographie, 74, 131–138.

Warren, B.E. and Trautz, O.R. (1930) The structure of hardystonite $Ca_2ZnSi_2O_7$. Zeitschrift für Kristallographie, 75, 525–528.

Manuscript received February 28, 2005
Manuscript accepted May 31, 2005
Manuscript handled by Yasuhiro Kudoh